

## Expanded View Figures

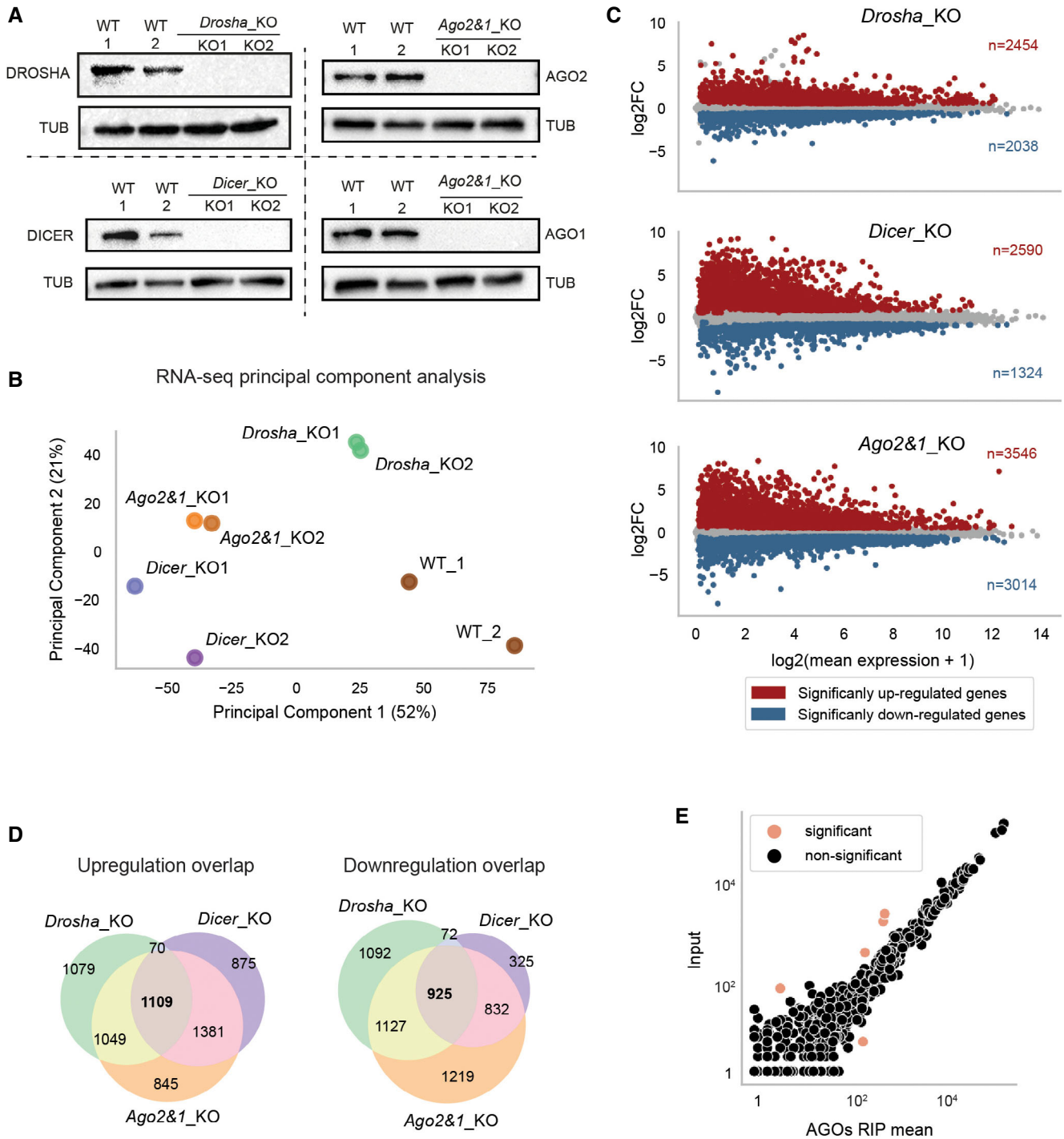


Figure EV1.

**Figure EV1. Gene expression is globally perturbed in *miRNA\_KO* mESCs.**

- A Immunoblot analysis of DROSHA, DICER, AGO1, and AGO2 in WT and their respective KO mESC lines. TUBULIN was used as a loading control. Representative blot of three independent experiments is shown.
- B PCA of gene expression as measured by RNA sequencing in *miRNA\_KO* and WT samples. Biological replicates are indicated with corresponding colors.
- C MA plots of the DGE analysis in *miRNA\_KO* mutants versus WT. Significant up- and downregulated genes are colored in red and blue, respectively.
- D Overlap of up- (left) and downregulated (right) genes in *miRNA\_KO* mESCs.
- E Comparison of miRNA loading for small RNA sequencing (Input) versus Argonaute2 & 1 (AGOs) RNA immunoprecipitation (RIP) and sequencing for all miRNAs. MiRNAs that show statistically significant difference between the two measured (adjusted *P*-value < 0.1) are highlighted.

Data information: In (C and E), significance in differential analysis was determined using an adjusted *P*-value threshold obtained from DESeq2 of 0.1. In (D), an adjusted *P*-value threshold of 0.2 was applied.

Source data are available online for this figure.

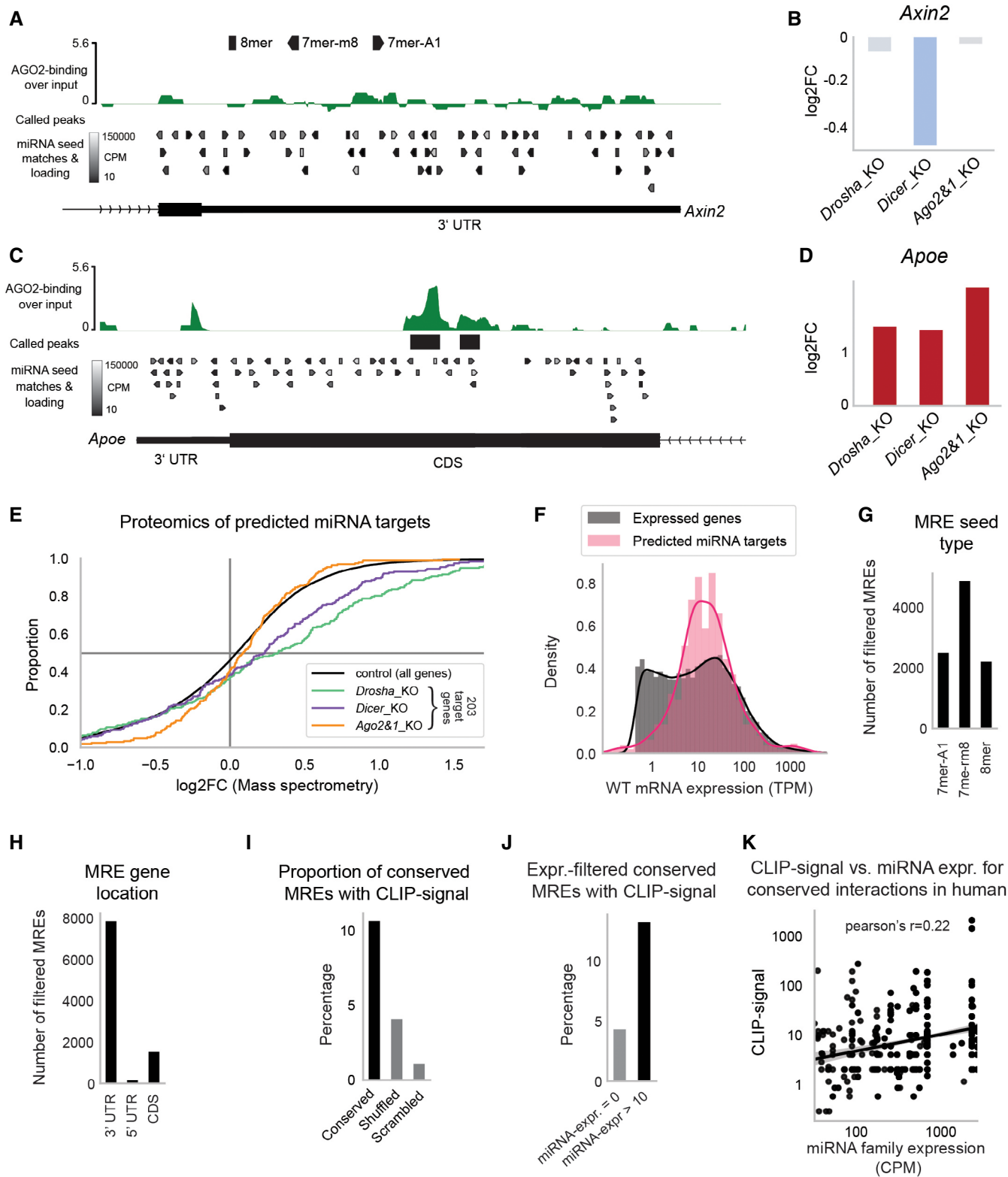


Figure EV2.

**Figure EV2. Characterization of predicted miRNA interactions.**

- A, B Example of integrated data for the *Axin2* gene with no evidence for functional interactions. For a more detailed subplot description, refer to the figure legend of Fig 1C and D.
- C, D No statistically significant AGO2-binding in 3'UTR of the *Apoe* gene, yet statistically significant binding to the CDS at a strongly expressed 8mer binding site along with a consistent upregulation in all three mutants. For a more detailed subplot description, refer to the figure legend of Fig 1C and D.
- E Cumulative distribution function of differential protein abundance as detected by SWAT-MS in *miRNA\_KO* mESCs. Of 759 predicted miRNA target genes, 203 (27%) were detectable in the SWAT-MS data and appear in the plot.
- F Expression distribution of predicted miRNA targets in comparison to expression of all genes (filtered by TPM >0.5 to improve comparability).
- G Number of filtered (see Fig 1A and B) miRNA response elements (MREs) grouped by the three most effective seed types 7mer-A1, 7mer-m8, and 8mer.
- H Number of filtered (see Fig 1A and B) MREs grouped by their location within the messenger RNA (3'UTR, 5'UTR, and CDS).
- I Conservation analysis of predicted interactions in hESCs. An interaction is considered conserved if a miRNA seed matching MRE is found in the 3'UTR of the human ortholog gene. Shown is the proportion of mESC-predicted interactions that have conserved MREs with associated cross-linking immunoprecipitation (CLIP)-seq reads in hESCs. As control, MRE search in hESCs was performed with shuffled and scrambled miRNA sequences.
- J Similar to (I), but only interactions with miRNA expression above 10 CPM (and = 0 CPM for control) were considered. miRNA expression was evaluated on a per-family basis, corresponding to the seed-match binding logic.
- K Correlation of hESC miRNA expression with the number of CLIP-seq reads in hESCs for human-conserved interactions (see Fig EV2I). Only interactions with at least one CLIP-seq read and at least 10 CPM miRNA expression are considered. miRNA expression is shown on a family basis (expression of miRNAs with the same seed is summed).

Data information: In (E), Student's *t*-test was applied to determine the significance of increased protein abundance for 203/759 miRNA targets ( $P < 0.0051$  for every mutant). In (K), Pearson correlation was calculated,  $P < 1e^{-50}$ . Source data are available online for this figure.

**Figure EV3. Validation of predicted miRNA targets.**

- A MiRNA loading in Argonaute2 &1 (AGOs) and number of predicted target counts for top five loaded miRNA clusters.
- B Loading of miRNAs in AGOs, highlighting *miR-290-295* cluster members.
- C *MiR-290-295\_KO* strategy and genomic validation. Top: Schematic representation of the paired CRISPR/Cas9 KO approach for the generation of *miR-290-295\_KO* cluster mESC lines. Genomic loci of miRNAs are indicated by blue boxes. Red lines mark sgRNA target sites. Primers for screening of the genomic deletion are indicated by pink half-sided arrows and pink lines show PCR products. Bottom: Genomic PCR screening of *miR-290-295\_KO* mESCs. Three screening primers, one around the 5' cut site, one around the 3' cut site, and one around the entire KO region (O) were used, as annotated at the top part of the subfigure. Expected amplicon sizes are denoted below the lanes. An X denotes no expected product.
- D Quantitative real-time PCR for representative *miR-290-295* members in WT and *miR-290-295\_KO* mESC lines. Expression levels were normalized to RNU6 in three biological replicates.
- E Cumulative distribution function of differential expression in *miR-290-295\_KO* for different gene groups, similar to Fig 3B. Colored log2FoldChange (log2FC) distributions correspond to different identification methods for miR-290-295 target genes based on different datasets (see Materials and Methods section). *Integrative approach* refers to the 360 *miR-290-295*-targeted genes out of the 759 miRNA target genes that have been identified in the integrative analysis of this paper (Fig 1A). *Lowly upregulated genes* are those that show a log2FC between 0.1 and 0.5 in all three mutants. *Low-up genes + integrative filtering* used the same set of genes but filtered for AGO2-binding to one of three strongly expressed *miR-290-295* members.
- F Quantitative real-time PCR showing relative expression levels of four predicted *miR-290-295* targets and two *miR-290-295* non-targets normalized to the control genes *Rrm2* or *Gapdh* in *Droscha\_KO Dicer\_KO* and *miR-290-295\_KO* mESCs.
- G Immunoblot analysis of TFAP4 after transfection of miRNA mimics (miR-291a-5p, miR-291a-3p and miR-291a-5p + miR-291a-3p combined) in *Droscha\_KO* mESCs. LAMINB1 was used as a loading control. Blot is a representative image of three biological replicates. Bottom: Bar graph showing quantification of TFAP4 intensity, normalized to LAMINB1 and relative to the WT sample in three biological replicates.

Data information: In (D), statistical significance for RT-qPCR of miR-290-295 members was assessed using a 2-way ANOVA test. \*\*\*\* $P < 0.0001$ . In (F), RT-qPCR bar graphs show relative expression of miR-290-295 targets and non-targets based on arbitrary units and normalized to a housekeeping gene (*Rrm2* or *Gapdh*) for three biological replicates. *P*-values were generated using a *t*-test comparing each value to the WT. \**P*-value < 0.05, \*\**P*-value < 0.01, and \*\*\**P*-value < 0.001. In G, bar graphs show mean intensity of TFAP4 signal  $\pm$  SD normalized to LAMINB1. Values are relative to the negative control mimic, which was set to 1. *P*-values were calculated using a Student's *t*-test comparing each value to the WT. \**P*-value < 0.05, \*\**P*-value < 0.01.

Source data are available online for this figure.

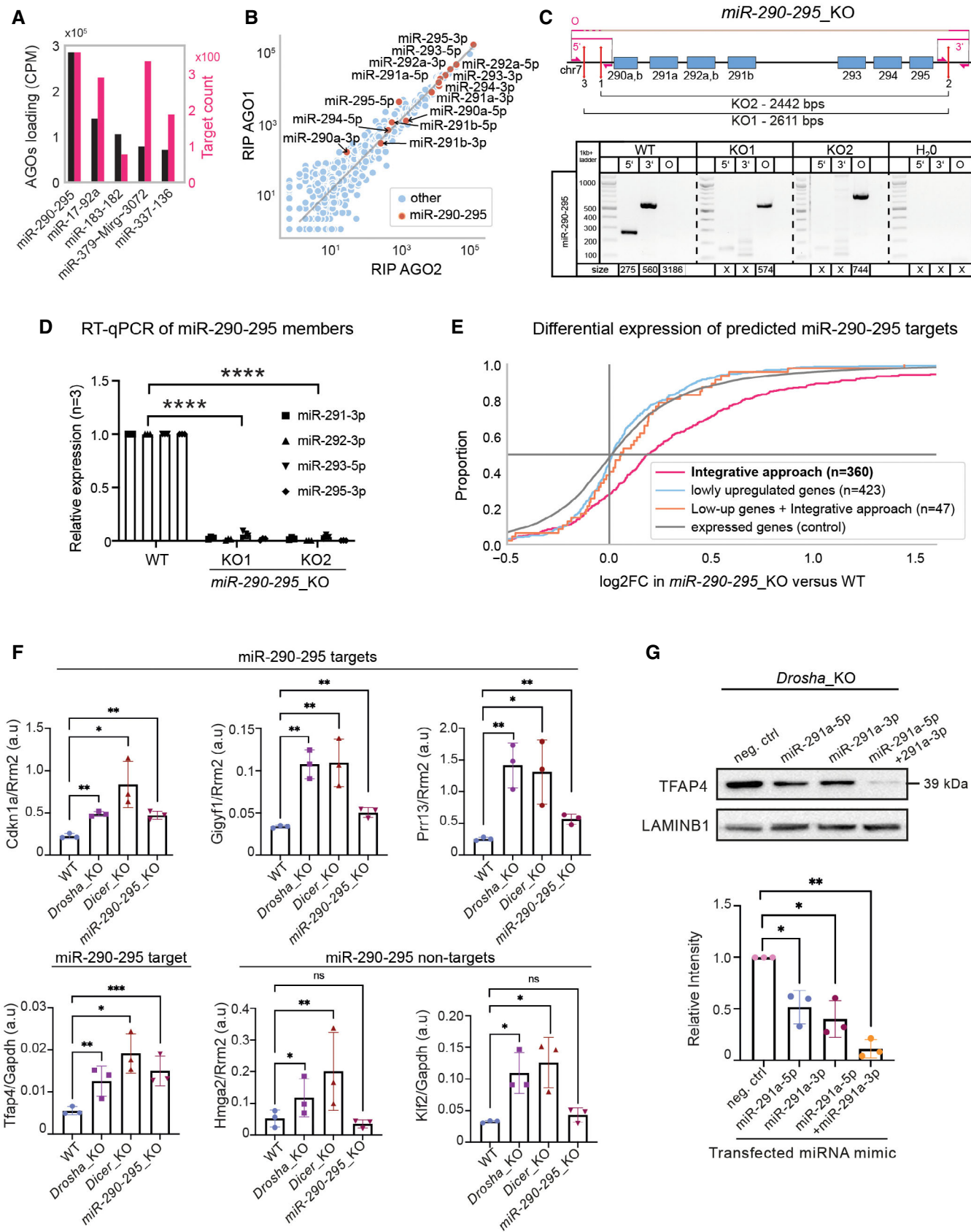


Figure EV3.

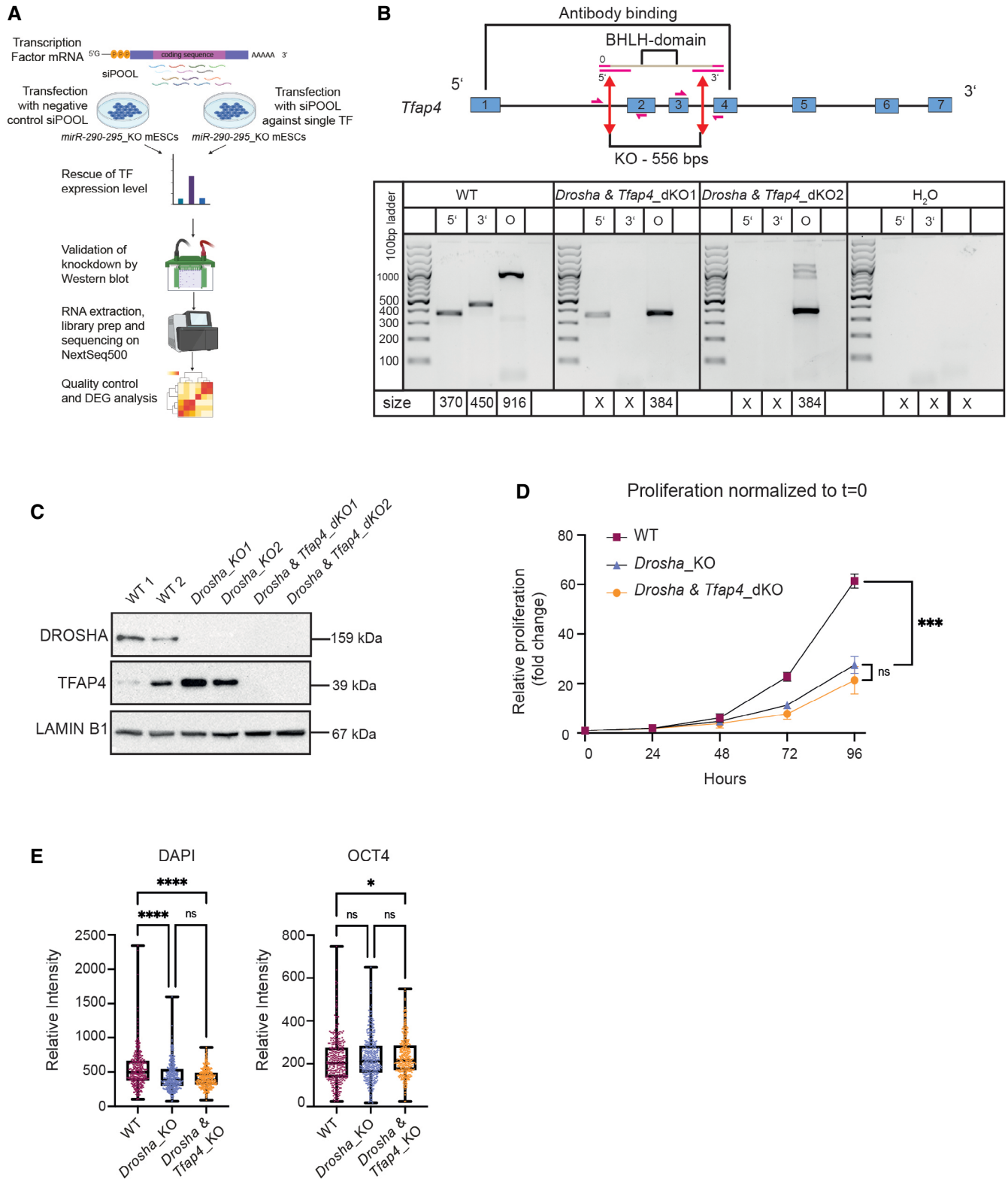


Figure EV4.

**Figure EV4. Depletion of *Tfap4* is not sufficient to rescue multiple *Drosha*\_KO phenotypes.**

- A Schematic representation describing the workflow to rescue TFAP4 expression by treating *mir-290-295*\_KO mESCs with pool of siRNAs (siPOOL) targeting *Tfap4*. Transfected cells were harvested and analyzed on the transcriptomics level using RNA-seq. Illustrations were extracted from BioRender.com.
- B Top: Schematic representation of the paired CRISPR/Cas9 approach used to establish a functional *Tfap4* knockout in *Drosha*\_KO mESCs. *Tfap4* exons are shown as blue boxes. Red double-sided arrows indicate the sites of Cas9 sgRNA binding. Pink arrows show binding sites of the primers used for knockout validation by genomic DNA PCR. Bottom: Genomic PCR screening of *Drosha* & *Tfap4*\_KO mESCs. Three screening primers pairs were used: one pair amplifies around the 5' cut site, one around the 3' cut site and one around the entire KO region (O) (see schematic representation above). Expected amplicon sizes are denoted below the lanes. An X denotes no expected product.
- C Western blot validation of *Drosha* & *Tfap4*\_KO clones. Immunoblot analysis of TFAP4 and DROSHA protein expression in WT, *Drosha*\_KO and *Drosha* & *Tfap4*\_KO. LAMINB1 was used as a loading control.
- D Proliferation assay in WT, *Drosha* KO and *Drosha* & *Tfap4*\_KO mESCs over 96 h. Relative change in proliferation is plotted for WT and KO cells as a mean of three biological replicates.
- E Quantification of DAPI and OCT4 fluorescence signal intensity in WT, *Drosha*\_KO and *Drosha* & *Tfap4*\_KO mESCs. The central band represents the median relative intensity for each genotype. The boxes represent the interquartile range and the whiskers represent the maximum and minimum relative intensity values.

Data information: In (E), box plots show nuclear intensity of OCT4 and DAPI in ~ 300 cells per genotype. *P*-values were generated using ordinary one-way ANOVA. \**P*-value < 0.05 and \*\*\*\**P*-value < 0.0001.

Source data are available online for this figure.

## Funding Information – Author Query

**AUTHOR:** Please check that the funding details given below match the details given in the Acknowledgement and provide any missing funder details. In compliance with certain funding agencies (e.g., US Department of Energy), please add the FundRef DOI(s), which can be found, for example, at: <http://www.wiley-vch.de/fundref/>

1) Please check that the funding details given below list all funding agencies and grant numbers given in the Acknowledgement and provide any missing funders and funder DOIs where required by you funding agency with the proof corrections.

2) Please check that the funder agency name and DOI is provided according to the official FundRef listing.

FundRef funding agency name	FundRef Doi	Grant number
örderung der Wissenschaftlichen Forschung" > Schweizerischer Nationalfonds zur Förderung der Wissenschaftlichen Forschung (SNF)	10.13039/501100001711	310030_196861, 31003A_173120, 182880
Open access funding provided by Eidgenössische Technische Hochschule Zurich		